Geotech Geol Eng (2024) 42:3491–3514
https://doi.org/10.1007/s10706-023-02740-x

ORIGINAL PAPER

Investigating Pore Water Pressure Development in Paste Backfill Under Conditions Mimicking Field Loading

Zubaida Al-Moselly · Mamadou Fall

Received: 2 August 2023 / Accepted: 28 December 2023 / Published online: 23 January 2024

Abstract This paper presents and discusses the outcomes of an experimental study aimed at investigating changes in pore water pressure (PWP) in cemented paste backfill (CPB) materials incorporating polycarboxylate ether-based superplasticizer (PES). The research mimics real-world backfill field curing conditions, encompassing factors such as thermal (T; field curing temperatures), hydraulic (H; drainage conditions), mechanical (M; field vertical stress), and chemical (C; presence or absence of PES) factors. Utilizing a developed THMC backfill curing system, controlled THMC experiments were conducted to assess the impact of these factors and their interactions on pore water pressure (PWP) in CPB with or without PES. Results reveal that both individual THMC factors and their interactions significantly affect PWP development within CPB. The study also highlights the impact of PES on PWP in CPB, showing that adding 0.125% of PES can lead to a reduction in pore water pressure values by approximately 50% after 28 days of curing. Moreover, the results obtained demonstrated the effectiveness of the experimental THMC test techniques developed in this study in successfully mimicking field-like loading conditions, substantiating their usefulness for subjecting laboratory CPB samples to realistic loading scenarios in the field. These findings are of great importance for the mining industry and backfill designers, providing technical insights into complex THMC interactions affecting PWP in CPB-PES. Understanding these relationships is vital for optimizing CPB and barricade design, ensuring structural integrity, enhancing mine productivity, and guiding future research on numerical models for PWP prediction across all CPB structures.

Keywords Cemented paste backfill · Tailings · Superplasticizer · Pore water pressure · Barricade · THMC · In-situ conditions

1 Introduction

An innovative method for managing large quantities of solid mining waste (tailings) and supporting underground mining is to use cement paste backfill (CPB), which is used to backfill underground mine cavities (stopes) to prevent surface subsidence and stope collapse, increase mine productivity and significantly control the environmental challenges that arise from surface tailings disposal, such as acid mine drainage and groundwater contamination (Fall et al. 2010a, b;

Z. Al-Moselly · M. Fall
Department of Civil Engineering, University of Ottawa, 161 Colonel by, Ottawa, ON K1N 6N5, Canada
e-mail: Zalmo047@uottawa.ca

M. Fall (✉)
Department Chair, Department of Civil Engineering, University of Ottawa, 161 Colonel by, Ottawa, ON K1N 6N5, Canada
e-mail: mfall@uottawa.ca

Wu et al. 2014; Aldhafeeri and Fall 2017; Cao et al. 2018; Jiang et al. 2019; Yilmaz et al. 2022; Zhang et al. 2022a, b; Chai et al. 2023; Sari et al. 2023). CPB is an engineered mixture consisting mainly of 70–85 wt% tailings from milling or processing operations, 3–7 wt% hydraulic binder, and fresh and/or mine-processed water (Yilmaz et al. 2003; Belem et al. 2006; Li et al. 2020; Roshani and Fall 2020; Haruna and Fall 2022). CPB is transported from the paste plant to mine stopes through a pipeline system by pumping or gravity (Orejarena and Fall 2008; Ercikdi et al. 2010; Wang and Qiao 2019; Sari et al. 2022). Mix fluidity is an important factor in the feasibility and the economic efficiency of delivering high-density CPB mix to underground stopes. Consequently, a high-performance water-reducing admixture, also known as a superplasticizer, is often added to the CPB mix to improve its fluidity (i.e., prevent pipe blockages and minimize material segregation) and thus facilitate its transport. In addition, the addition of this admixture can lead to an increase in the mechanical strength of CPB materials (Ercikdi et al. 2010; Ouattara et al. 2017; Haruna and Fall 2020; Al-Moselly et al. 2022).

In mining operations, each stope's footprint is constrained by a designed barricade (retaining structure) usually located at the base of the stope to prevent the long column of fresh CPB materials, over ten vertical meters of continuous CPB pour, from flowing into adjacent stopes or active mining operations until the CPB reached its desirable strength (Helinski et al. 2007, 2011; Cui and Fall 2018b; Alainachi et al. 2022). Preserving the stability of barricades during the backfilling process is paramount in any paste-fill operations. The disastrous implications of barricade failure have a severe social (i.e., threats to mining personnel lives) and economic impact (i.e., additional cost caused by the delay in production) on mining operations (Shahsavari and Grabinsky 2016; Fang and Fall 2019, 2020, 2021). The primary technical risk causing barricade failure occurs when the developed pressure by the CPB materials is greater than the designed pressure of the barricades (Cui and Fall 2016, 2017a,b). The pressure applied to the designed barricades is greatly dependent on several complex interactions, including the effect of the self-weight of the CPB mass, dissipation of pore water pressure and the related development of the effective stress within the CPB structure (Helinski et al. 2006). The significant increase in the positive pore water pressure of the CPB materials at early ages represents a significant threat to the stability of the barricades (Lu and Fall 2018; Zhao et al. 2020). The dissipation of the excess positive pore water pressure coupled with the development of negative pore water pressure (suction) or the reduction of water content in the CPB materials leads to a strength gain (i.e., increase in the effective stress) and thus leads to the required hardening stage in the CPB materials and early opening of barricades (Ghirian and Fall 2013a, 2015).

Moreover, in underground stopes, CPB material is also subjected to complex interactions involving the thermal, T, (e.g., variation in mine temperature due to the depth and geological conditions of the mine, self-heating due to the presence of sulphide minerals, heat generated from cement hydration), the hydraulic, H, (e.g., drained conditions, partially drained, undrained conditions), the mechanical, M, (e.g., variation in the stresses applied to the CPB structure which largely depends on the stope geometry, stope depth, self-weight of the CPB, backfilling rate, cement content, designed pressure of the barricades, in situ stress conditions) and the chemical, C, (e.g., cement hydration, superplasticizer) factors (Fall et al. 2010b; Helinski et al. 2011; Wu et al. 2012; Ghirian and Fall 2014, 2015; Wu et al. 2019; Al-Moselly and Mamadou 2022; Yan et al. 2023). Therefore, because of the unique characteristics of each mine operation and stope conditions, it is crucial to understand the development of pore water pressure within the CPB structure under various field conditions for designing a stable and cost-effective CPB structure and reducing mine cycles (i.e., early opening of barricades).

Many studies have been carried out in the past to assess the pore water pressure development within the CPB materials (e.g.Helinski et al. 2007; Shahsavari and Grabinsky 2015, 2016; Ghirian and Fall 2013b, 2015; Al-Moselly and Mamadou 2022). But, as of now, despite notable advancements in comprehending pore water pressure (PWP) evolution in CPBs, almost all previous studies have focused solely on investigating the individual effects of some influencing factors (e.g. binder hydration, binder type, backfill height) on CPB PWP development. For example, Helinski et al. (2007) investigated the reduction in pore water pressure due to the cement hydration process using an analytical model and was experimentally verified using two different types of tailings. It was observed that the volume changes resulting from cement

hydration caused significant changes in the pore water pressure, and the reduction in pore water pressure significantly depends on the cement-tailings mixture, the amount of water consumed during the cement hydration process, material stiffness, and the porosity of the material. Shahsavari and Grabinsky (2015 and 2016) numerically predicted the pore water pressure variation within the backfill stope under various material properties, backfill depth and weight. Ghirian and Fall (2013b), 2015) investigated the effect of drainage conditions and filling rate on the development of positive pore water pressure (PWP) and suction within the CPB materials with time. They found that the pore water pressure significantly increases at an early age as the filling rate increases, and the application of both drainage and curing under stress on the CPB materials at the early hours of curing causes a quick development of suction. Shahsavari et al. (2023) carried out backfill column experiments and their results indicate that the rapid filling rate of the column has an impact on the development of pore water pressure in the CPB and that the highest pore water pressures occur at the end of filling. Min et al.'s (2023) experimental studies conclusively demonstrate the substantial influence of binder type on suction (negative pore water pressure) development in CPB. Specifically, their findings reveal that CPB incorporating (sulpho) aluminate-based cements exhibited elevated suction levels and more pronounced self-desiccation.

However, to date, no studies have addressed the impact of coupled thermal-hydraulic-mechanical-chemical (THMC) factors on the development of PWP in CPB. Research and knowledge gaps exist regarding the coupled effects of field temperature variations (T factor), pressure or stress applied to CPB (e.g. overburden pressure, backfill rate) (M factor), drainage conditions (drained and undrained) (H factor) and additives used in the preparation of CPB (e.g. superplasticizer) (C factor) on the development of PWP sure in CPB. This gap in knowledge and research needs to be filled given the importance of PWP in the design of backfill and barricade structures, as discussed above. Therefore, the objective of this study is to investigate the development of PWP within CPB materials containing superplasticizer by mimicking real field conditions, encompassing various coupled THMC interactions. By delving into these interconnected factors, this research seeks to shed light on how they collectively impact PWP in the CPB. Comprehending these interconnections is essential to enhance CPB and barricade designs, guarantee structural soundness, improve mining efficiency, and guide upcoming research on numerical models to predict PWP development in CPB structures.

2 Experimental Program

2.1 Materials

2.1.1 Tailings

The tailings used in this experimental investigation were synthetic silica tailings (ST), a non-reactive silica powder of 99.8% quartz (SiO_2). A grain size distribution analysis was carried out, and the obtained grain size distribution curve is presented in Fig. 1. This figure shows that the grain size distribution curve of the silica tailings is close to the average of nine Canadian mine tailings. Also, from this curve, the values of D_{10}, D_{30}, and D_{60} were 1.9, 9.0, and 31.5 µm, respectively. Therefore, the synthetic silica tailings can be classified as medium-sized tailings (35–60 wt% of less than 20 μm particles) (Landriault 2001). Synthetic silica tailings were utilized to meticulously regulate the chemical and mineralogical compositions, eliminating uncertainties in the analysis and interpretation of results. This approach ensures precision by avoiding the presence of reactive chemical elements found in natural tailings, which might otherwise interact with cement and potentially skew the outcomes. Tables 1 and 2 present the physical properties and the chemical composition of the used synthetic silica tailings, respectively.

Table 1 Physical properties of the tailings used in this study

Element	G_s	D_{10}	D_{30}	D_{50}	D_{60}
Unit	–	µm	µm	µm	µm
ST	2.7	1.9	9.0	22.5	31.5
Average of 9 natural Canadian mine tailings	–	1.8	9.1	20.0	30.8

Gs specific gravity

Table 2 Mineralogical composition of the silica tailings

Concentration (wt.%)	Ingredient (symbol)								
	SiO_2	Fe_2O_3	Al_2O_3	TiO_2	CaO	MgO	Na_2O	K_2O	Loss on ignition
	99.8	0.035	0.05	0.02	0.01	< 0.01	< 0.01	0.02	0.1

Table 3 Chemical and physical properties of the binder used

Element (%)	SO_3	Fe_2O_3	Al_2O_3	SiO_2	CaO	MgO	Relative density	Specific surface (m^2/g)
PCI	3.8	2.7	4.5	18.0	62.8	2.6	3.2	1.3

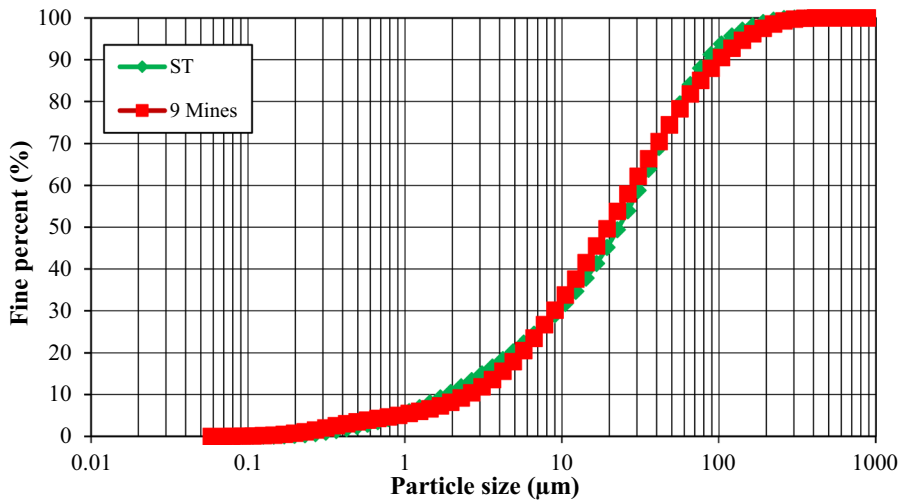

Fig. 1 Grain size distribution of the silica tailings used and that of the average of nine natural mine tailings in Eastern Canada

2.1.2 Binder and Water

Portland cement (PC) type 1 (PCI) was utilized in this study as the hydraulic binder. PC is the most common type of binder used in CPB technology, as it is widely available worldwide, making it a practical and accessible option for paste backfill operations worldwide. In addition, PC is compatible with a variety of mineral admixtures and additives, making it possible to tailor the paste backfill mix to specific mine conditions. The chemical and physical properties of the PCI are provided in Table 3. Tap water was used in this study for mixing tailings and the binder.

2.1.3 Chemical Additives

A polycarboxylate ether-based superplasticizer type was chosen in this experimental study as a water-reducing additive. The polycarboxylate ether-based superplasticizer, commonly used in the concrete industry, is characterized as the most effective superplasticizer type for its dispersing mechanism (Ouattara et al. 2017, 2018). Polycarboxylate ether-based superplasticizer exhibit good compatibility with a wide range of cements, including ordinary Portland cement, blended cements, and others (Haruna and Fall 2022). Polycarboxylate ether-based superplasticizer has steric hindrance forces, which arise from the comb structure of high molecular weight (i.e., the main backbone molecules, produced from the polymerization of carboxylic acid groups (polycarboxylate), are linked to the other polycarboxethlene side chains) to prevent agglomeration of cement particles (Yoshioka et al. 1997; Björnström and Chandra 2003; Papayianni et al. 2005). The polycarboxylate ether-based superplasticizer, denoted by PES, used in this study is a commercial solution that meets ASTM C 494/C 499 M requirements for Type A water-reducing and Type F high-range water-reducing admixtures (BASF 2015).

2.2 Sample Preparation

The CPB with PES (CPB-PES) mixtures were prepared by adding the necessary amounts of tailings to the specified percentage by weight of PCI (4.5%) and mixing them together for about 2 min in a mechanical mixer. While continuing the mixing, the specified percentage of polycarboxylate ether-based superplasticizer (PES = 0% and 0.125%) and the measured amount of tap water were added and thoroughly mixed for 7 min to obtain a homogenized CPB-PES material. The measured amount of water was calculated using a water-to-cement ratio (*w/c*) of 7.35 in all mixes. After mixing, freshly prepared CPB-PES mixtures were poured into the pressure cell cylinders explained below and cured under various field THMC curing conditions for specific curing times. The experimental variables (i.e., mixing composition and curing conditions) are listed in Table 4 below.

2.3 Description of the THMC Backfill Curing System

The curing system employed in this study for simulating the influence of various THMC factors that may affect the pore pressure development and dissipation within the CPB-PES structure, originally developed at the Ottawa University by Ghirian and Fall (2013b), 2015), is additionally altered and explained in detail in Al-Moselly et al. (2022), and only a brief summary is given in this section. The curing system is capable of considering the influence of various THMC factors, such as the evolution of PWP (in this manuscript, the term PWP refers to positive pore water pressure), suction (negative pore water pressure), cement hydration, self-weight (overburden pressure) caused by mine stope filling processes, temperature variation, and drainage conditions (drained, undrained, and partially drained). The modified pressure cell setup for both drained and undrained conditions is schematically presented in Fig. 2. The modified

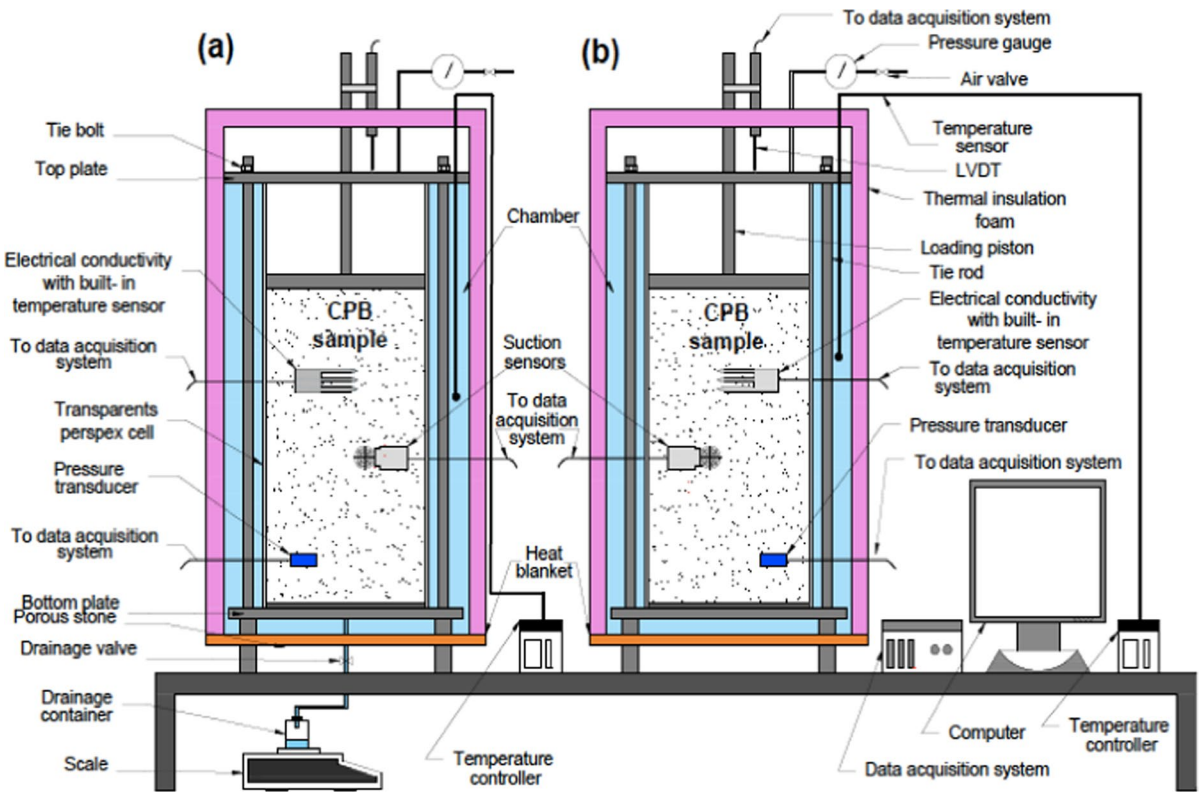

Fig. 2 Schematic diagram of the pressure cells arrangement: **a** drained condition, and **b** undrained condition. (modified from Ghirian and Fall 2015)

Table 4 Summary of specimens mixing composition and curing conditions

Sample name	Tailings type	Binder type (C)	PES content (%) (C)	Curing stress (M)	Drainage condition (H)	Curing temperature (T)	Curing time (day)
Control-UD-0.0% PES	ST	PCI	0	Stress-free	UD	20 °C	0.5, 1, 3, 7, 28
Control-UD-0.125% PES	ST	PCI	0.125	Stress-free	UD	20 °C	0.5, 1, 3, 7, 28
THMC-D-0.125% PES	ST	PCI	0.125	Field stress[a]	D	Field temp.[b]	0.5, 1, 3, 7, 28
THMC-PD-0.125% PES	ST	PCI	0.125	Field stress[a]	PD	Field temp.[b]	0.5, 1, 3, 7, 28
THMC-UD-0.0% PES	ST	PCI	0	Field stress[a]	UD	Field temp.[b]	0.5, 1, 3, 7, 28
THMC-UD-0.125% PES	ST	PCI	0.125	Field stress[a]	UD	Field temp.[b]	0.5, 1, 3, 7, 28

pressure cell consists of an acrylic plastic mould with a diameter of 101.6 mm (4 inches) and a height of 304.8 mm (12 inches). Two cover plates were placed at the top and bottom of the cylinder, with three stainless steel tie rods to hold the cylinder and the two plates together. The bottom plate is provided with a drainage valve to control the drainage conditions (i.e., water flow), and an axial loading piston is attached to the top plate to simulate the backfilling processes (curing under stress) of the mine stope by applying compressed air pressure into the CPB-PES specimen. The modified pressure cell is enclosed by a temperature-controlled chamber to simulate the non-isothermal curing conditions.

In addition, the modified pressure cell is equipped with a series of pressure gauges and pressure regulators to control the gradual application of the air pressures and various sensors to monitor the change in temperature, volumetric water content, and electrical conductivity (EC), as shown in Fig. 2. The development of suction and PWP were continuously monitored during the specified curing time using MPS-6 dielectric water potential sensor and Omega PX309 pressure transducers, respectively. The testing and monitoring program, including the details of the used sensors, are further discussed in Sect. 2.5 below.

2.4 Applied THMC Curing Conditions and Monitoring Program

The experimental program was planned to investigate the development of PWP of the CPB-PES samples with different initial compositions prepared according to the procedures explained above under various field curing conditions described below and summarized in Table 4.

2.4.1 Mechanical Curing Conditions (Curing under Applied Vertical Field Pressure)

The amount of the vertical field pressure applied to the CPB during placement into the stope and throughout its operational lifespan is intrinsically affected by the variation in the backfilling rate, stope depth, stope geometry, and cement content from mine to mine (Thompson et al. 2009; Al-Moselly and Mamadou 2022). Miscalculations of the specific stresses applied to the CPB materials and the related development of pore water pressure increase stope cycle times and can cause serious barricade failure. Accordingly, to address the critical importance of variation of the field pressures applied to the CPB materials, the curing system used in this study is designed to simulate and investigate the development of PWP of the CPB-PES materials cured under the application of field vertical pressure or overburden pressure. The in-situ pressure data applied to the CPB-PES materials in this study were obtained from field measurements of a mining operation collected by Thompson et al. (2009) for a long hole stope of 32 m in height and a footprint of 28 × 19 m. Detailed vertical pressure and the equivalent backfill rate and height applied to the CPB-PES specimens with time are summarized in Table 5. Note that no pressure was applied to the

Table 5 Pressure application scheme and the corresponding equivalent CPB height

Elapsed time	Applied vertical pressure (kPa)	Equivalent height (m)	Equivalent filling rate (m/hrs)
start	-	-	-
2 h	20	1.00	0.50
4 h	35	2.00	0.50
6 h	55	3.00	0.50
8 h	60	3.20	0.40
10 h	80	4.30	0.43
12 h	90	4.80	0.40
1 d	100	5.38	0.22
1.5 d	125	6.66	0.19
2 d	150	7.92	0.17
3 d	250	13.25	0.18
4 d	400	21.41	0.22
5 d	450	24.00	0.20
6 d	600	32.00	0.22

CPB-PES sample at the first 2 h; after that, a gradual air pressure increased to 600 kPa with an average filling rate of 0.26 m/h after 3 m height.

ST silica tailings, *PES* polycarboxylate ether-based superplasticizer, [a] simulated field curing stress (vertical pressure), [b] simulated field curing temperature; *D* drained, *PD* partially drained, *UD* undrained conditions, *PCI* Portland cement type I, *C* chemical factor, *M* mechanical factor, *H* hydraulic factor, and *T* thermal factor.

2.4.2 Hydraulic Curing Conditions

The experimental testing program was designed to assess the impact of drainage conditions on the evolution of pore water pressure in CPB-PES materials over time. In the field, the drainage capacity of the CPB mass is contingent upon various factors, including the permeability of the CPB materials, geological characteristics of the surrounding rock (such as fractures in the rock mass), and groundwater conditions in the mine. For instance, undrained drainage conditions may arise when the surrounding rock mass is solid and lacks fractures. Conversely, drained (D) conditions may manifest when the surrounding rock mass is extensively fractured. Furthermore, the permeability of CPB materials is not only affected by curing time and temperature, but also by factors such as mix components, binder content, and fineness of tailings particles (Fall et al., 2009).

To account for the diverse drainage conditions that a CPB mass may encounter in the field, this study adopts three drainage scenarios: undrained conditions (UD), partially drained conditions (PD), and drained (D) conditions. To replicate undrained conditions in the experimental setup of this study, the drainage valve at the bottom plate (see Fig. 2) remained closed throughout the entire curing period. Conversely, to emulate drained conditions, the drainage valve was fully opened during this time. On the other hand, to model partially drained conditions, the drainage valve was partially opened for approximately 1.5 days during curing, facilitating the drainage of around 50% of the water from the CPB. It is important to emphasize that PD conditions are the most likely to occur in the field and occur when the drainage conditions of the CPB mass fall between UD and D conditions.

2.4.3 Thermal Curing Conditions

Isothermal (20 °C) and non-isothermal curing temperatures (reflecting field conditions) were adopted to investigate the influence of temperature variations on the evolution of pore water pressure in CPB-PES over time. In the field, the backfill mass experiences non-isothermal curing, primarily attributed to heat generated during binder hydration within the backfill structure. Figure 3 illustrates temperature variations within a 30 m-high stope backfilled with CPB material containing 4.5% binder content, as predicted by Nasir and Fall (2009) and Wu et al. (2013) using numerical modeling. Sets of CPB specimens were cured in accordance with the temperature profile depicted in Fig. 3 to assess the influence of non-isothermal field curing conditions and THMC on the pore water pressure development in CPB-PES. Essentially, the application of the temperature profile illustrated in Fig. 3 when curing CPB samples allows us to discern the role of in-situ backfill temperature in the progression of pore water pressure within the backfill. The experimental set-up described in Fig. 2, comprising a heating blanket and a controller, was used to systematically, precisely raise and control the temperature over time. This configuration facilitated the application and regulation of a gradual temperature increase. The incorporation of the heating blanket and controller allowed for the replication of temperature-time

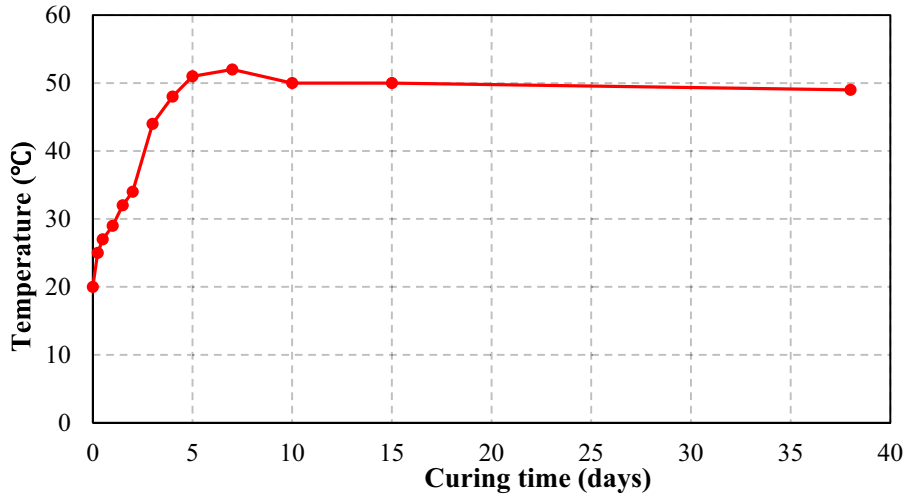

Fig. 3 Predicted field temperature inside a 30 m stope height backfilled with CPB material of 4.5% binder content (from Nasir and Fall 2009 and Wu et al. 2013)

profiles observed or measured in the field CPB structure, ensuring consistent curing conditions for the CPB samples housed within the chamber. Curing the CPB-PES materials in these conditions allows for observation of the self-desiccation process within the CPB-PES structure and the development of pore water pressure.

2.4.4 Chemical Curing Conditions

Various sensors were deployed in the modified curing system to examine the effect of the chemical factor on the development of PWP in the CPB-PES materials with time. The experimental program was designed to monitor, compare, and analyze the influence of the chemical composition of the CPB materials (i.e., tailings, cement, and water) on the development of pore water pressure in the CPB materials cured under various curing conditions with the aim to quantify the influence of the chemical additive (i.e., polycarboxylate ether-based superplasticizer) on the evolution of negative and positive pore water pressure of the mixtures with time. The chemical processes are mainly driven by the binder or cement hydration and the chemical interactions between the CPB-PES mix components, including tailings, binder, mixing water, and polycarboxylate ether-based superplasticizer. The various sets of curing conditions considered in this study program, as shown in Table 4, allow us to study the effect of chemical processes on the development of pore water pressure of the CPB-PES materials cured under various curing conditions (i.e., temperatures, free and field curing stress, and drainage conditions).

2.5 Testing and Monitoring Programs

2.5.1 Pore Water Pressure Monitoring

The development of pore water pressure in the CPB-PES samples cured under various field conditions was monitored with time using various sensors. The development of negative pore water pressure (suction) in the CPB-PES samples cured under various field conditions with time was monitored using MPS-6 dielectric water potential sensors with a range of −9 to −100,000 kPa and an accuracy of ± (10% of reading + 2 kPa) from −9 to 100 kPa. Following the proposed CPB-PES sample poured in the modified pressure cell curing cylinder, the recording of negative pore water pressure (suction) began at specific time intervals. The suction results were recorded using an applicable data logger.

The development of PWP in the CPB-PES samples cured under various field conditions was monitored with time by an Omega PX309 pressure transducer inserted inside the CPB-PES sample. The Omega PX309 pressure transducer can measure the pore water pressure between − 15 to + 15 PSI and ± 0.25% accuracy. The PWP monitoring data were recorded using a computer data acquisition system.

2.5.2 *Electrical Conductivity and Temperature Monitoring*

The process of cement hydration and the chemical interactions between the CPB-PES mix components (tailings, binder, mixing water, and polycarboxylate ether-based superplasticizer) were monitored using a 5TE temperature sensor mounted in the pressure cell to record the electrical conductivity (EC) and temperatures of the CPB-PES sample with time. The 5TE temperature sensor can measure the electrical conductivity with an accuracy of ±0.1 from 0 to 23 dS/m and monitor the evolution of temperature within the CPB-PES samples with an accuracy of ±1 °C and a range of −40°Cto 60 °C. The electrical conductivity data reveals the ion concentration and ion mobility changes in the CPB-PES specimen, which can help in assessing the progress of ions in the pore fluid of the CPB-PES mixture (Li and Fall 2016). The 5TE temperature sensor was connected to an applicable data logger to store the monitoring data with time.

2.5.3 *Volumetric Water Content Monitoring*

The volumetric water content (VWC) of the backfill specimens was recorded with time using the 5TE temperature sensor, which is the same sensor used to monitor the EC. The 5TE is capable of measuring VWC in a range of percentages from 0 to 100% with an accuracy of ±15% from 40 to 80. The VWC data reveals the percentage of water consumed by the ongoing cement hydration process of the CPB-PES sample.

2.5.4 *Determination of Physical Properties and Microstructure*

The influence of the THMC processes on the development of PWP was further investigated by examining the pore structure (e.g., void ratio, porosity, density) of the CPB-PES with time. Gravimetric water content ($\omega\%$) and bulk density (γ) tests were performed on the CPB-PES samples at different curing times (0.5, 1, 3, 7, and 28 days) according to ASTM D2216-10 and ASTM D7263-09, respectively. The development of the samples' physical properties and pore structure, including void ratio (e) and porosity (n), were also measured and assessed with time.

In addition, to assess the types and the relative quantities of hydration products generated in the CPB-PES samples, thermogravimetric (TG and DTG) analyses were performed on selected cement paste samples (w/c = 1; to mimic the high water content of CPB). The paste samples were prepared and cured in similar conditions as the CPB specimens. The tests were executed using a thermogravimetric analyzer, which implies continuous monitoring and recording of weight loss, heat flow, and temperature changes in the sample at a rate of 10 °C per minute up to 1000 °C.

3 Results and Discussion

3.1 Effect of THMC Factors on the Evolution of Pore Water Pressure in the CPB-PES

Figure 4 presents the evolution of the PWP within the CPB materials cured under various simulated field curing factors or conditions with time, respectively. It shows the combined effects of the thermal (T), hydraulic (H), mechanical (M), and chemical (C) factors on the development of PWP in the CPB containing PES and cured under THMC factors (THMC-D-0.125% PES) compared to the CPB material without PES and cured under conventional laboratory (Control-UD-0.0% PES) conditions (i.e., stress-free, undrained, and cured under room temperature of 20 °C). During the early hours of curing, the PWP value within the CPB material for the THMC-D-0.125% PES sample was initially recorded at 2.3 kPa, then progressively increased to reach the peak values of 34 kPa after around 4.5 h of curing, whereas the PWP values within the CPB material for the control sample (Control-UD-0.0% PES) monotonically decreased with time from the initial recorded reading of 4.2 kPa. This initial increase in PWP observed in samples subjected to conditions reproducing real field scenarios has been observed in numerous field investigations of CPB structures (e.g., Thompson et al. 2009; Doherty et al. 2015).

The increase in the PWP values in the THMC-D-0.125% PES sample can be attributed to the following mechanisms: (i) the fluid behaviour of the fresh CPB-PES materials at the early hours of curing,

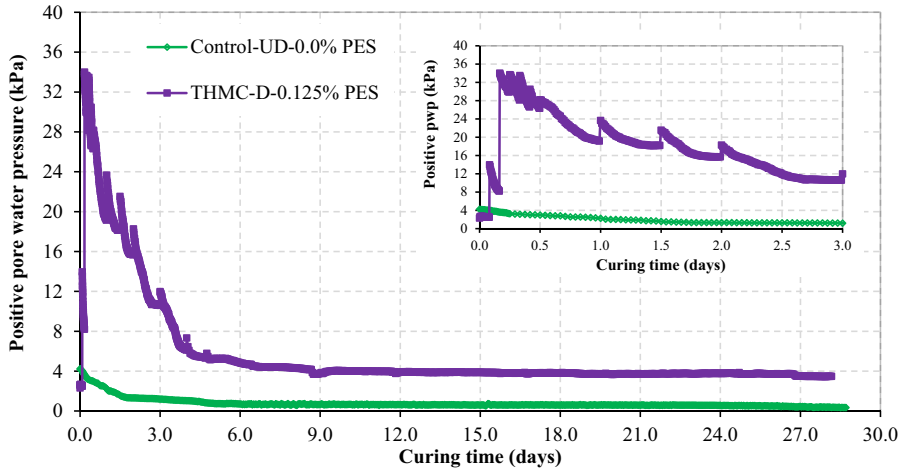

Fig. 4 PWP evolution within the CPB-PES material cured under various THMC factors with time

resulting from large amounts of unbonded water (Simms and Grabinsky 2009); (ii) the weak microstructure of the CPB sample at the very early hours of curing, which is caused by the pressure applied to the CPB sample. The application of pressure induces microcracking and displacement at the contact points between the cement hydration products (Ghirian and Fall 2016). Indeed, the microstructure of cemented paste, when subjected to excessive curing stress during its early stages, exhibits weakness. Consequently, the points of contact between the hydration products of cement are vulnerable to microcracking and displacement (Zhou and Beaudoin 2003); (iii) the application of pressure in the early hours induces the sample to behave like a fluid and therefore increases the PWP (Ghirian and Fall 2015; Al-Moselly et al. 2022). Similarly, applying stress to the CPB-PES sample at the early hours of curing rearranges the solid particles (i.e., tailings and cement) and speeds up the release of additional free water, resulting in higher PWP measured (Ghirian and Fall 2016; Chen et al. 2021). The monitoring results of the volumetric water content tests for the THMC-D-0.125% PES and the control sample (Control-UD-0.0% PES) presented in Fig. 5 demonstrate the higher amount of free water in the THMC-D-0.125% PES sample in the first few hours of curing compared to the control sample; (iv) the self-weight settlement and rearrangement of solid particles at the very early age of curing led to a decrease in the volume of voids (Yilmaz et al.

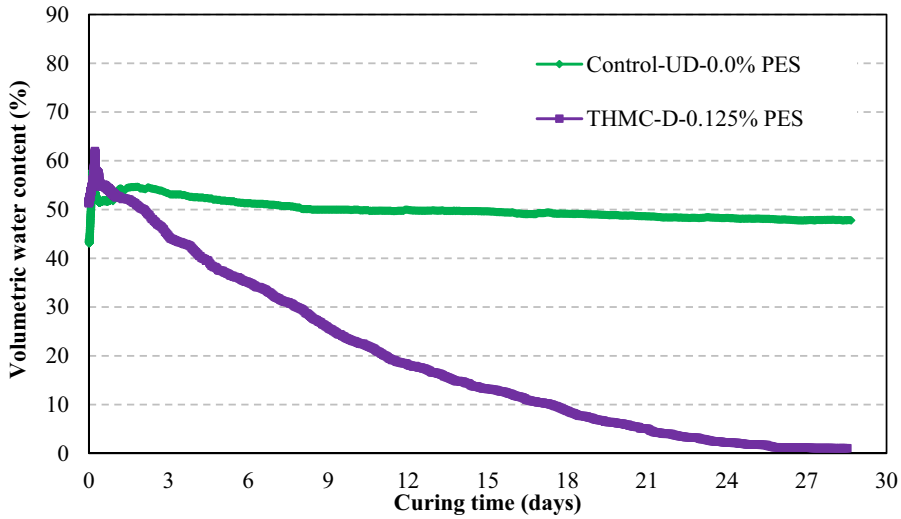

Fig. 5 Volumetric water content monitoring results with time for different CPB-PES samples

2012). The decrease in void volume can be observed by the results of the void ratio tests for the THMC-D-0.125% PES compared to the Control-UD-0.0% PES samples, as shown in Fig. 6. In addition to the above mechanisms, the increase in the PWP values in the THMC-D-0.125% PES sample at the early ages of curing can also be accredited to the dispersion effect of polycarboxylate ether-based superplasticizer (PES). Superplasticizers derived from carboxylic compounds, such as PES, instigate two distinct repulsive forces between cement particles: (i) electrostatic repulsion arising from the negative charges attributed to the carboxylic group, and (ii) steric repulsion linked to the extensive polymer chains present in the compound (Huang et al. 2022; Haruna and Fall 2022).The repulsive forces between the cement particles induced by the addition of PES to the CPB mixture release the water trapped by tailing particles and cause a delay in the setting time at early ages, which in turn is associated with the higher amount of free water, and thus the increase in the PWP values (Ercikdi et al. 2010; Mangane et al. 2018; Haruna and Fall 2022; Al-Moselly et al. 2022). The effect of adding polycarboxylate ether-based superplasticizer to the CPB mixture on the evolution of pore water pressure is further investigated and analyzed in the following subsections of this study.

Furthermore, Fig. 4 shows that after reaching maximum PWP values, the PWP values for the THMC-D-0.125% PES sample begin to dissipate over time. This observed initial rise in pore water pressure, succeeded by a gradual decline (dissipation) in the pore water pressure of the CPB samples (THMC-D-0.125% PES) subjected to coupled THMC loading conditions, aligns well with findings from various field studies of CPB masses (e.g., Thompson et al. 2009, Doherty et al. 2015, Wang et al. 2023). This consistency reinforces the efficacy of the experimental THMC testing techniques pioneered in this study. These techniques successfully replicate field-like loading conditions, substantiating their utility in subjecting laboratory CPB samples to realistic field loading scenarios. This dissipation of the excess PWP is attributed to the chemical shrinkage (i.e., net volume reduction) caused by the reaction of cement with water in the ongoing cement hydration process and the related formation of hydration products (Hua et al. 1995; Helinski et al. 2006, 2007), i.e. the self-desiccation process (Al-Moselly et al. 2022). Helinski et al. (2007) demonstrated that the cement hydration process produces a significant reduction in PWP values (self-desiccation) in CPB materials with time, and that the rate of PWP reduction (i.e., the amount of water consumed during cement hydration) depends on various factors such as cement composition, cement surfaces exposed to water for reactions, and the different amounts of water used in each reaction. This self-desiccation is also responsible for the time-dependent decrease in PWP observed in the control sample. Specifically, as the hydration reaction advances, capillary water (free water) undergoes a progressive transformation into chemically bound

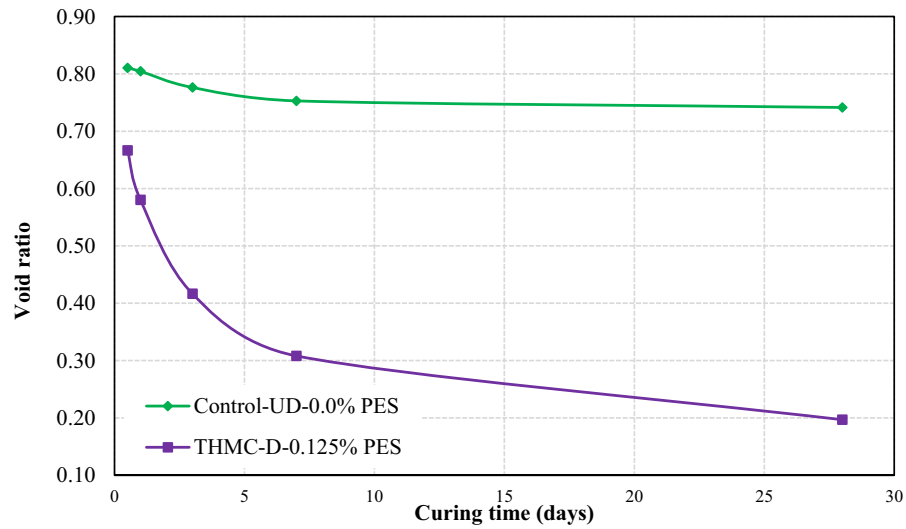

Fig. 6 Changes in the void ratio of CPB-PES with time under various THMC curing conditions

water within the solid phase. This transformation results in the formation of hydrates with a volume less than the combined volume of the original cement and water. Consequently, this process leads to a decrease in the water content within the CPB matrix, a phenomenon known as self-desiccation. The reduction in water content contributes to a corresponding decrease in PWP and could result in the development of suction within the CPB material or mass (Cui and Fall 2017c). This explanation is also in line with the results of suction monitoring of the CPBs studied presented in Fig. 7. This figure illustrates the influence of THMC factors on the development of suction within the CPB-PES materials with time. It should be stressed that the sensors used to monitor suction (MPS-6) and those used to monitor PWP (Omega PX309) were not placed at the same depth in the CPB cell. The Omega PX309 was located near the bottom of the cell, while the suction sensor was placed in the middle of the cell. Figure 7 shows that as CPB curing age increases, suction in CPB-PES materials increases, and the rate of increase in the sample cured under simulated field conditions (THMC-D-0.125% PES) is significantly higher than the control sample. In other words, self-desiccation is more intense in CPB cured under coupled THMC conditions. The higher suction observed in the sample cured under simulated field conditions can be attributed to the following mechanisms: (i) curing the CPB-PES sample under field elevated temperatures (thermal factor) expedite the cement hydration process, which leads to a higher consumption of water with time (Fall et al. 2010b). This faster cement hydration is experimentally demonstrated by the results of the monitoring of electrical conductivity (EC) at the early hours of curing presented in Fig. 8. This figure shows an intensification of the chemical reactions of cement hydration for the THMC-D-0.125% PES sample in comparison to the control sample. As illustrated in Fig. 8, the trends in electrical conductivity (EC) development among the analyzed samples exhibit distinct characteristics, beginning with an initial ascent to a peak value, followed by a subsequent decline, eventually stabilizing. The initial increase is attributed to a surge in ion concentration resulting from the chemical reaction of the binder (Thottarath 2010). The subsequent decline can be attributed to several factors, including the formation of hydration products of the binder, depletion of free water, and the transformation of capillary pores (Lea 1970). At this later stage, the CPB is marked by intensified crystal formation and the establishment of a more robust crystalline network through crystal bonding. Consequently, the ions in free water encounter a more convoluted path as they traverse the capillary pores within the CPB (Morsy 1999). It can be seen from Fig. 8 that the THMC-D-0.125% PES sample reached its peaks at 2.6 mS/cm after about 3 h of curing, whereas the control sample (Control-UD-0.0% PES) peaks at 4.6 mS/cm after about 4 h of curing, which indicates a higher rate of cement hydration process in the CPB-PES sample cured under THMC factors (Al-Moselly et al. 2022); (ii) the dissipation of excess PWP caused by the drained conditions (hydraulic factor) and the

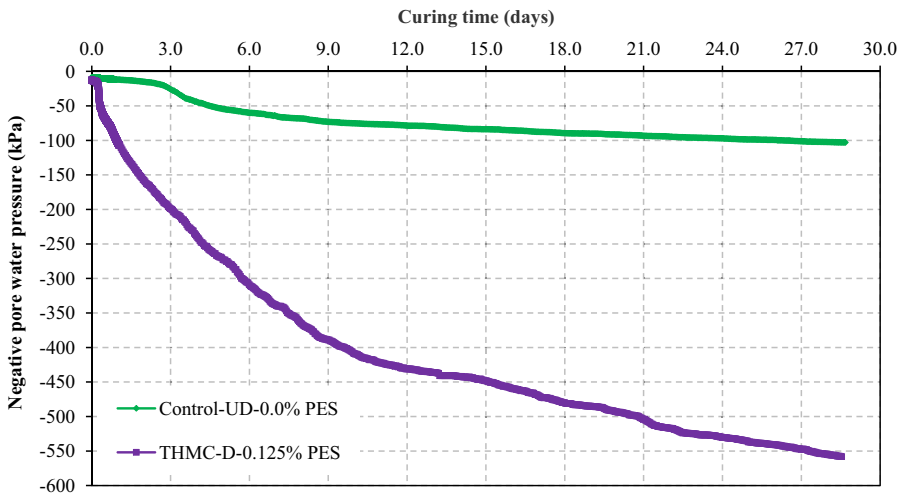

Fig. 7 Negative pore water pressure (suction) evolution within the CPB-PES material cured under various THMC factors with time

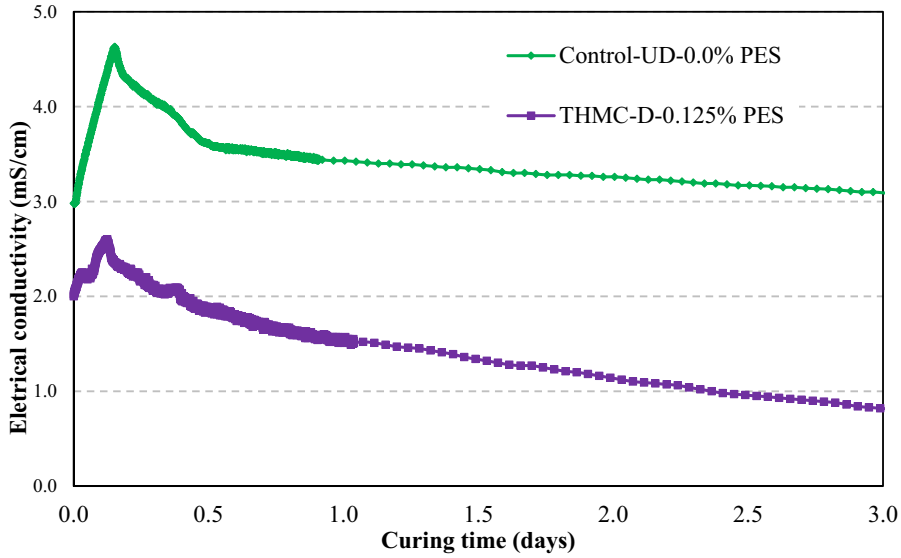

Fig. 8 The EC evolution of CPB-PES with time under various THMC curing conditions

related development self-desiccation results in less water in the pores (i.e., partially empty). The presence of menisci in these partially empty pores generates capillary tension within the pores and thus increases suction in the CPB sample (Bentz 2008). Also, allowing excess PWP to drain from the CPB-PES sample at an early age significantly contributes to binder hydration due to the rapid development of self-desiccation, and consequently, higher suction (Fall et al. 2010b). The influence of drainage conditions on the evolution of pore water pressure in the CPB mixture is further investigated and discussed in the following subsections of this research, (iii) curing the CPB-PES sample under field pressure (mechanical factor) significantly increases the water drainage, which results in more dissipation of excess PWP, and thus, higher suction (Yilmaz et al. 2009; Ghirian and Fall 2016), and (iv) the favouring of ionic diffusion produced by the addition of polycarboxylate ether-based superplasticizer (chemical factor) increases the cement hydration process, and therefore increases consumption of water, which in turn increases the suction in the CPB-PES sample (Haruna and Fall 2020).

Moreover, comparison of the results from PWP and suction monitoring, as depicted in Figs. 4 and 7, reveals that self-desiccation triggered CPB desaturation or suction development at an earlier stage in the upper or middle section of the CPB cell than at its base. This discrepancy arises from the influence of gravity and/or applied pressure, causing a higher accumulation of interstitial water at the bottom of the cell as opposed to the top or middle regions. This observation is consistent with several field or numerical studies of PWP development or self-desiccation in CPB structures under undrained conditions (e.g., Cui and Fall 2018a).

3.2 Effect of Drainage Conditions on the Evolution of pore Water Pressure within the CPB-PES

Figure 9 shows the influence of various drainage conditions (undrained, drained, and partially drained conditions) on the evolution of the PWP within the CPB-PES samples cured under various THMC factors. It is found that during the early ages (i.e., the first 24 h), the PWP increased with time for all samples, regardless of the drainage conditions. The mechanisms responsible for this initial increase in PWP have already been explained above. Moreover, the measured PWP values within the undrained (THMC-UD-0.125% PES) sample is significantly higher than both the drained and partially drained CPB-PES samples (Fig. 9). For instance, allowing the water to drain during the early ages of curing reduced the PWP by 58% when compared to the undrained sample (THMC-UD-0.125% PES). This significant reduction in the PWP values in the samples subjected to drainage is attributed to the following factors: (i) the dissipation of excess pore water pressure resulted from the drainage of water from the CPB-PES materials. The

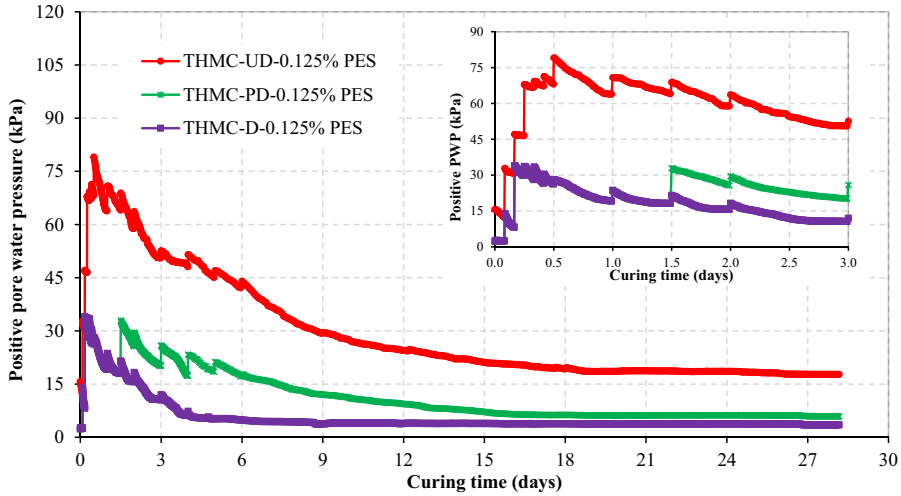

Fig. 9 Influence of drainage conditions with time on the PWP within the CPB-PES samples cured under various THMC factors

water contained in CPB-PES materials can be drained through the interconnected pore, and as the excess water drains away, the PWP decreases (Ghirian and Fall 2015). The volumetric water content monitoring test results, as illustrated in Fig. 10, provide a clear demonstration of the reduction in the volume of water with time for both samples. The drained sample (THMC-D-0.125% PES) exhibits a higher reduction compared to the undrained sample (THMC-UD-0.125% PES). (ii) Consolidation plays a vital role in pore water reduction in the CPB-PES with time (Helinski et al. 2007; Yilmaz et al. 2012). As the CPB-PES undergoes consolidation caused by the self-weight of the CPB-PES materials and the vertical pressure applied to the sample, the excess water in the CPB-PES sample void spaces is forced out of the material, and thus the PWP decreases with time. This expulsion of water is confirmed experimentally by the results of water content determination presented in Fig. 11. Indeed, Fig. 11 exhibits the substantial reduction in the water content with time in the THMC-D-0.125% PES sample in comparison to the THMC-PD-0.125% PES and THMC-UD-0.125% PES samples. The decline in pore water pressure within CPB over time, resulting from a combination of processes such as consolidation and self-desiccation, has been consistently documented in various field investigations of CPB structures. An example is the study conducted by Hasan et al. (2013) in two operational stopes at the Raleigh mine in Western Australia,

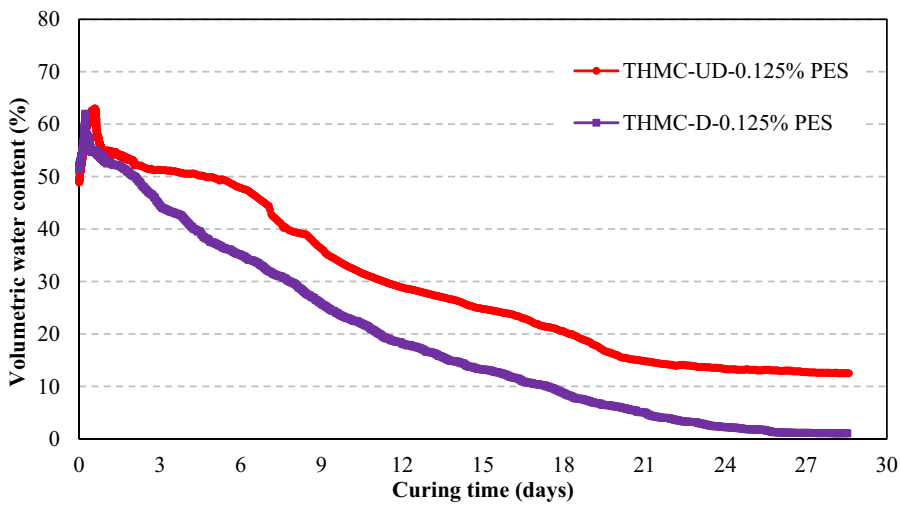

Fig. 10 Effect of drainage conditions on the volumetric water content of CPB-PES samples cured under THMC factors

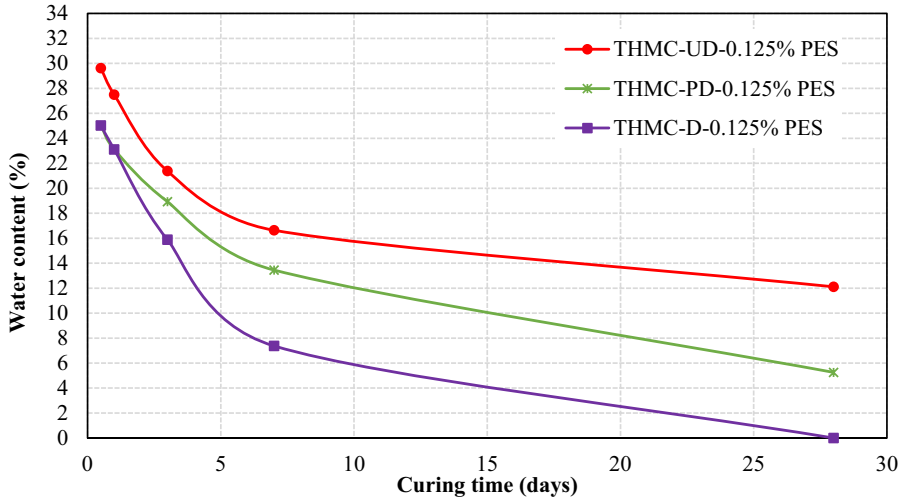

Fig. 11 Water content variation with time of the CPB-PES cured under various drainage conditions and THMC factors

which took place underground. The research by Hasan et al. revealed that the drainage system implemented effectively reduced significantly both the total horizontal stress and the pore water pressure within the backfill mass. This reduction was directly associated with the processes of backfill consolidation and self-desiccation. Their findings underscored the positive impact of a well-designed drainage system for CPB.

From a practical standpoint, these findings on the influence of drainage conditions on pore water pressure within CPB underscore the pivotal role of CPB possessing effective water drainage capabilities or the implementation of a robust drainage system. This is instrumental in improving both the mechanical stability of the backfill structure and the integrity of barricades in underground mines. Indeed, a CPB system with optimal water drainage ability, and/or a well-designed drainage system, significantly contributes to enhancing mechanical stability. This is achieved by mitigating PWP, facilitating better consolidation, and minimizing horizontal stress. Consequently, these improvements positively impact the stability of barricades within underground mines, ensuring the safety and integrity of mine workers and the overall mining infrastructure. Furthermore, the rapid reduction of stress facilitated by effective drainage is pivotal for the timely opening of barricades. This, in turn, holds substantial implications for the mining cycle and, consequently, the productivity of the mine. The accelerated stress reduction due to drainage not only improves the stability of the barricades but also plays a crucial role in expediting their opening, thereby optimizing the efficiency of the mining operations.

3.3 Effect of Superplasticizer on the Evolution of pore Water Pressure within the CPB-PES

The evolution of PWP within the CPB-PES is closely associated with the addition of chemical additives, such as superplasticizers. Figure 12 illustrates the contribution of polycarboxylate ether-based superplasticizer (PES) addition to the reduction of the PW of the CPB-PES material cured under various in-situ conditions (i.e., THMC) with time, respectively. From Fig. 12, it can be observed that at the early age of curing, the CPB sample containing 0.125% PES exhibited higher PWP compared to the CPB sample without PES. After that, the excess PWP buildup in the CPB sample containing 0.125% PES (THMC-UD-0.125% PES) is reduced and revealed lower values than the CPB sample without PES. The initial increase in the PWP values in the CPB sample containing 0.125% PES can be attributed to the primary function of the superplasticizer in dispersing the solid particles (tailings and cement), which leads to solid particles suspension and water release, which in turn results in higher PWP (Ercikdi et al. 2010; Haruna and Fall 2022). Previous studies demonstrate that when the superplasticizer is added to the CPB, it adheres to the cement particles' surface, creating a protective layer that inhibits or slows down the hydration process (Mangane et al. 2018; Haruna and Fall 2020; Al-Moselly et al. 2022; Cavusoglu and Fall

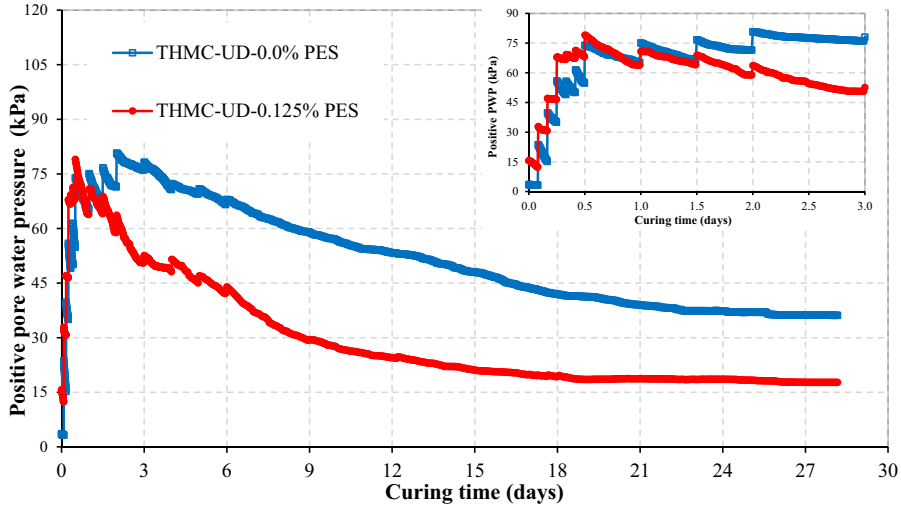

Fig. 12 Effect of polycarboxylate ether-based superplasticizer on the pore water pressure development of CPB cured under various THMC factors

2022; Yan et al. 2023). Delayed initial hydration of cement by superplasticizer has also been demonstrated in other types of cementitious materials (e.g., Sakai et al. 2006). This early retardation effect of PES causes the initial increase in the PWP values in the CPB sample containing 0.125% PES. Indeed, Fig. 13 confirms the initial increase in the moisture content (%) in the CPB sample containing 0.125% PES compared to the CPB sample without PES. In practical terms, the findings indicate that CPBs incorporating PES experience initially higher PWP levels compared to those without PES. This implies that, in real mine backfill operations, CPBs with PES may achieve their early-age stability later than counterparts prepared without PES, which could lead to a delay in barricade opening. Furthermore, it is noteworthy that backfills containing PES will exert increased pressure on barricades compared to those without PES. In essence, this suggests the necessity of constructing more robust barricades to support CPBs with PES during their initial stages of development. While the initial rise in PWP may have adverse effects on the total stress or the decrease in effective stress for CPB materials during early stages, it is crucial to underscore the significance of the initial delay induced by PES in prolonging the setting time of CPB materials. This becomes particularly pertinent when considering the transportation of backfill over extended distances and/or exposure to high-temperature curing conditions, a circumstance often encountered in deep mining

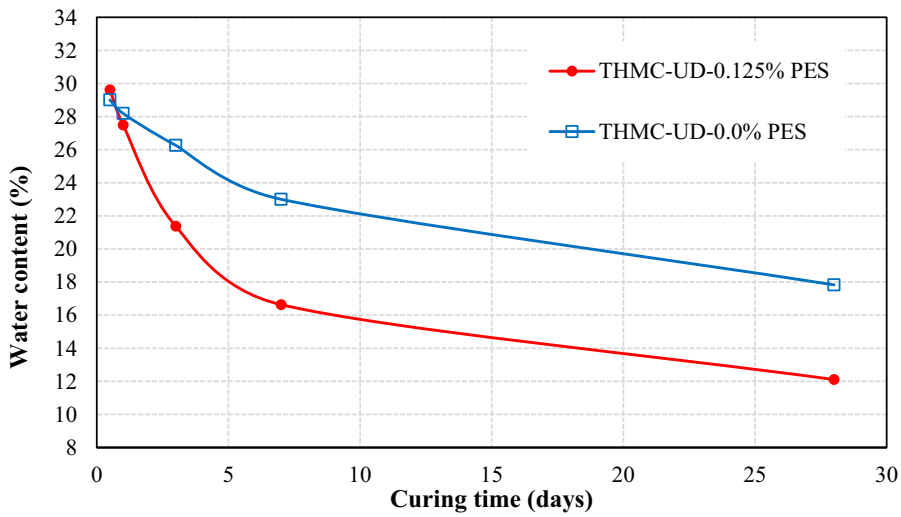

Fig. 13 Effect of incorporating PES in the CPB mixture cured under various THMC factors on the water content (%) with time

operations. Ensuring the seamless transportation of fresh CPB from the backfill plant to the stope (mine cavity) is imperative for the success of paste backfilling operations. The potential obstruction of pipelines, resulting from CPB with inadequate flow characteristics, carries substantial financial consequences for the mine.

Furthermore, Fig. 12 also shows that as the curing progresses and the peak pore water pressure values are reached in both samples, the PWPs gradually decline over time. As mentioned above, the sample containing 0.125% PES exhibited lower PWP than those without PES. It can be seen that the addition of 0.125% PES can lead to a reduction in pore water pressure values by approximately 50% after 28 days of curing. This is due to the higher precipitation rate of the hydration products caused by the ionic diffusion of PES, which enhances cement particle dispersion (Haruna and Fall 2020). This higher rate of cement hydration in the sample with PES is confirmed by the EC monitoring results presented in Fig. 14. This figure demonstrates that the EC in the CPB with 0.125% PES is lower than the EC in the CPB sample without PES after 28 days of curing (i.e., the ions in the sample with 0.125% PES have lower mobility than the sample without PES), which provide an indication of the intensifying rate in the hydration process and the associated cement hydration products (McCarter et al. 2003; Haruna and Fall 2020). This intensification of cement hydration and the resulting increase in hydration products are consistent with the TG/DTG analysis results of cement paste samples containing 0% and 0.125% PES dosages, which were cured for 7 days (Fig. 15). In Fig. 15, the first endothermic peak in the DTG curve, occurring between 100 and 200 °C, represents the rapid weight loss due to the evaporation of water and the disintegration of hydration products, such as ettringite, gypsum, carboaluminates, and C-S-H (Wang et al. 2016). The peak observed at 400 to 500 °C corresponds to the dehydroxylation of calcium hydroxide (CH), while the third peak at 650 to 750 °C is related to the breakdown of calcite (Fall et al., 2010a, 2010b). A comparison of the thermal analysis curves of the cement paste with 0% and 0.125% PES reveals that the specimen with 0.125% PES experiences a greater loss in the first and second peaks. This indicates that the presence of PES leads to the generation of more hydration products. This statement also in agreement with the experimental results concerning the variation in void ratio and dry density of CPB samples with 0.125% PES and without PES presented in Fig. 16. The results show lower void ratio values for the CPB sample made with 0.125% PES compared with the CPB sample without PES after 12 h curing. It can also be observed that after 12 h of curing, the dry density values of the CPB sample made with 0.125% PES are higher than those of the sample without PES due to the intensification of the binder hydration rate, which in turn leads to greater free water consumption and higher packing density of CPB materials over time (Ghirian and Fall 2013b, 2014; Al-Moselly et al. 2022).

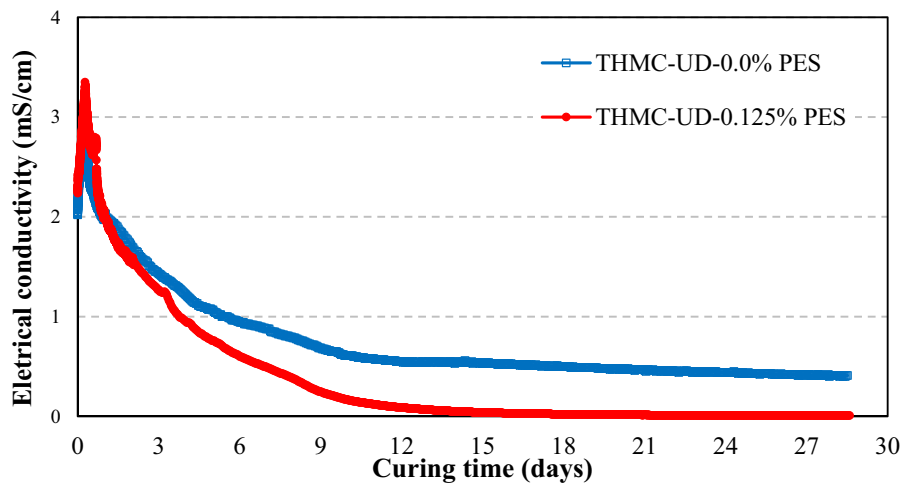

Fig. 14 Time-dependent variation in electrical conductivity of CPB materials cured under various THMC factors with different PES content

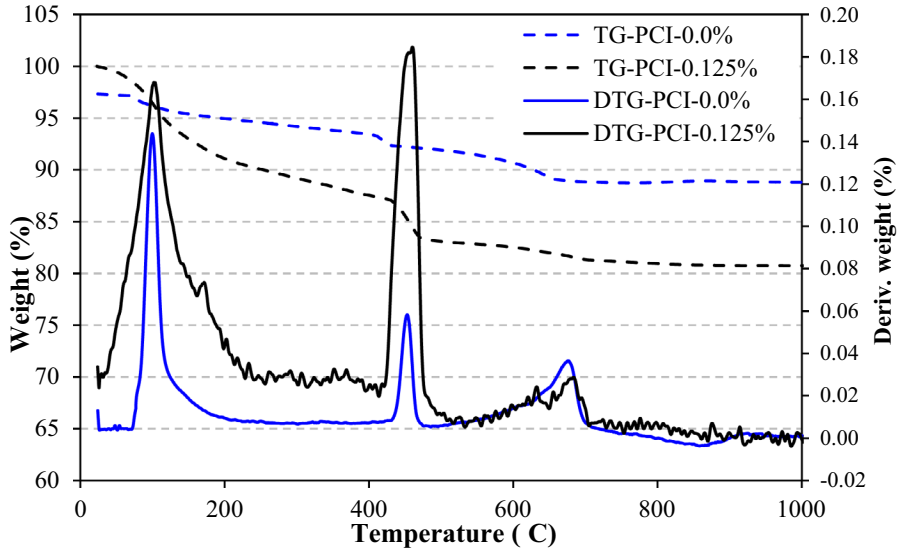

Fig. 15 TG/DTG diagrams for 7-day old cement paste with 0.125% PES and without PES.

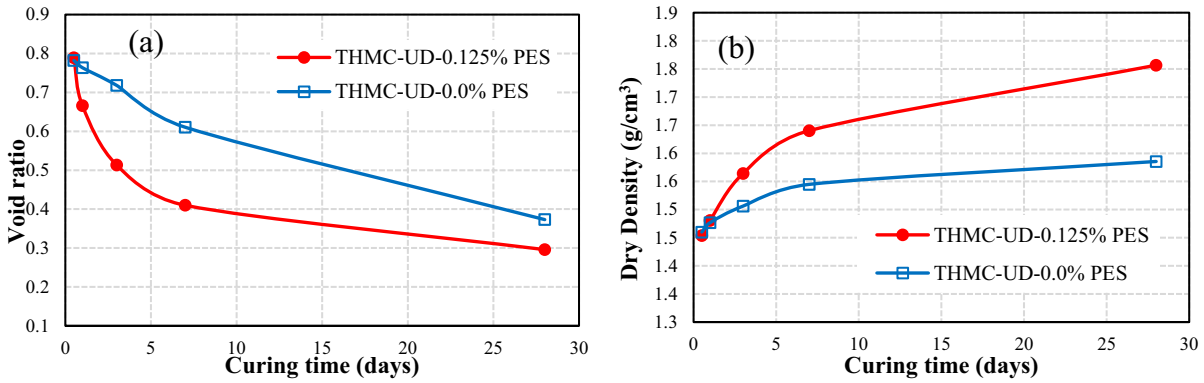

Fig. 16 Variation in the physical properties of CPB materials cured under various THMC factors with different PES content (a) void ratio; and (b) dry density

3.4 Coupled Development of the THMC Factors

The coupled effect of field conditions (i.e., the THMC factors) plays a crucial role in understanding the long-term performance and behaviour of CPB. The interplay between the in-situ conditions, such as temperatures, drainage conditions, stress, and chemical additives, significantly affects CPB materials' overall stability and durability. The complex interaction requires a thorough investigation to optimize CPB materials for cost-effective and sustainable applications. Figure 17a, b illustrate the interaction of the THMC factors and their effect on the PWP evolution within the CPB materials cured in drained and undrained drainage conditions, respectively. The THMC factors are simulated as follows: (i) the thermal factor (T) effect is simulated by the elevated temperatures (i.e., the non-isothermal field curing temperatures); (ii) the hydraulic factor (H) is represented by the PWP pressure (PWP) and volumetric water content (VWC); (iii) the mechanical factor (M) is simulated by the vertical field stresses applied to the CPB-PES materials; and (iv) the chemical factor (C) is simulated by the electrical conductivity (EC), which provides valuable insight into the progress of cement hydration processes and imitates the changes in chemical composition and reactions within the CPB mixture. It can be observed from Fig. 17a, b

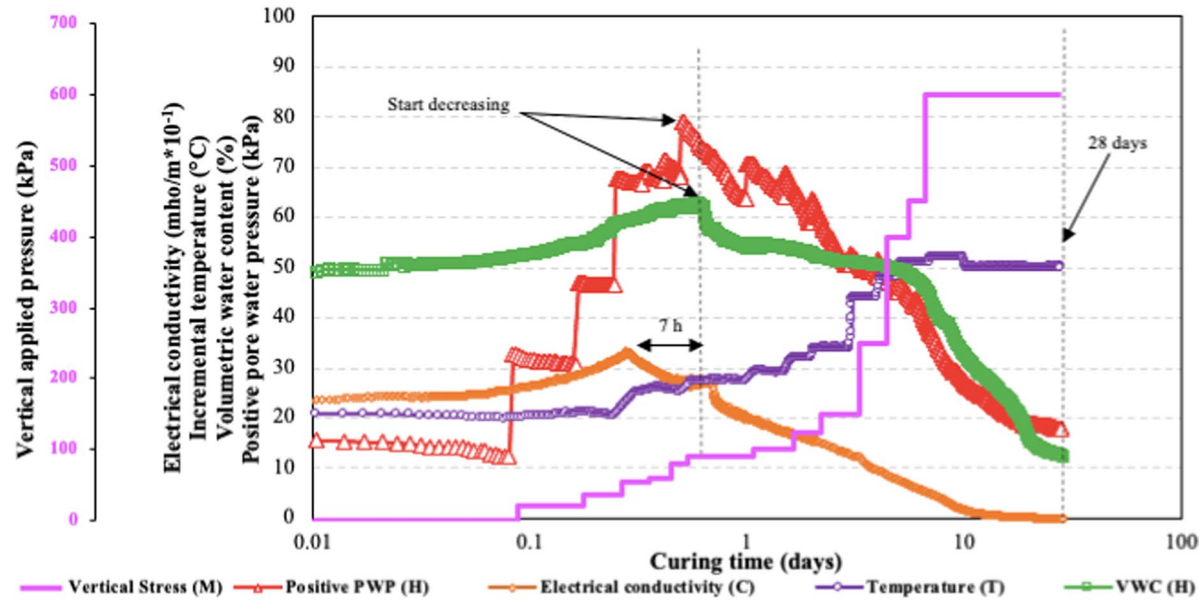

a) Undrained CPB-PES sample cured under various THMC factors (THMC-UD-0.125% PES).

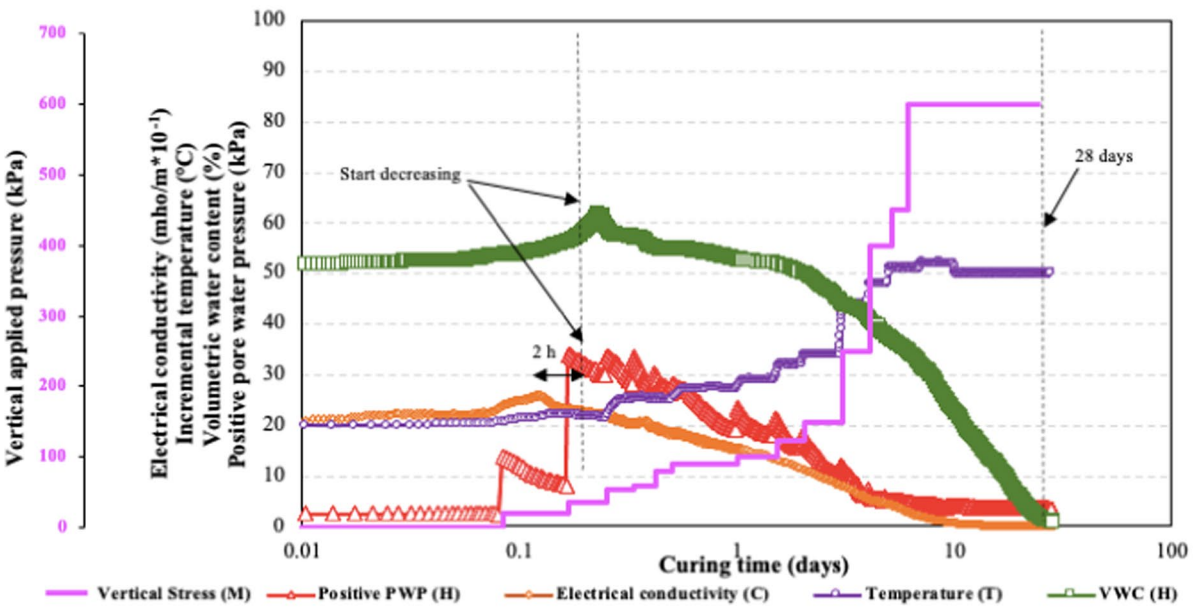

b) Drained CPB-PES sample cured under various THMC factors (THMC-D-0.125% PES).

Fig. 17 **a** Undrained CPB-PES sample cured under various THMC factors (THMC-UD-0.125% PES). **b** Drained CPB-PES sample cured under various THMC factors (THMC-D-0.125% PES). Coupled evolution of electrical conductivity, volumetric water content, negative pore pressure (suction), and pore water pressure (PWP) of CPB material with 0.125% PES with time.

that as the curing temperatures and vertical stresses increase, a notable effect is observed in the EC curve, which demonstrates a rapid acceleration in its values. This acceleration in the EC values reflects the increase in the cement hydration process within the CPB-PES mixture triggered by the coupled influence of applied pressure and elevated curing temperatures, which resulted from the release of heat generated during the cement hydration reactions (Haruna and Fall 2020), and curing the CPB-PES samples in non-isothermal curing temperatures. Concurrently, the PWP displays an upward trend, ultimately reaching its maximum value. This increase in the PWP values is directly linked to the VMC. It can be observed that the VMC exhibits a distinct behaviour, with its peak occurring approximately 7 h after the maximum values of EC are reached for the undrained sample (THMC-UD-0.125% PES). In contrast, the drained sample (THMC-D-0.125% PES) experiences a VMC peak approximately 2 h after reaching its maximum EC value. This time disparity suggests variations in water movement and consumption within the CPB-PES mixture, influenced by different drainage conditions, as explained earlier in subsection 3.2. After that, a noticeable decline in the VWC values in both samples occurs. This reduction in the VWC for both samples is reflected in the observed rapid decrease in the PWP values. This diminution in VWC and PWP is intricately linked to water consumption during cement hydration (self-desiccation). In the undrained samples, this process is the primary contributor, whereas in drained samples, the decrease in VWC and PWP results from a combination of self-desiccation and water removal through drainage. Consequently, the reduction in the pore water (i.e., the dissipation of excess PWP) began in an earlier curing time for the THMC-D-0.125% PES sample compared to the THMC-UD-0.125% PES sample due to the drainage conditions. For instance, the PWP values for the THMC-D-0.125% PES sample start to decrease at approximately 4 h of curing, whereas the PWP values for the THMC-UD-0.125% PES sample begin to decrease after approximately 12 h of curing time.

4 Summary and Conclusions

This paper significantly advances our understanding of the development and evolution of pore water pressure (PWP) in cemented paste backfill (CPB) containing a polycarboxylate ether superplasticizer (CPB-PES) under the influence of various field THMC factors (thermal, T, hydraulic, H, mechanical, M, and chemical, C) during the curing process. These factors include field non-isothermal curing temperature of the backfill mass (T factor), in situ drainage conditions (H-factor), in situ vertical stress applied to the CPB mass (M-factor) and the presence or absence of superplasticizer in the CPB mix (C-factor). By considering the impact of these multiple THMC factors, the study provides a comprehensive and holistic view of how these factors individually and collectively influence the PWP development and evolution over time, which is crucial for the safe and economical design of cemented tailings backfill and barricades structures, in other words for the safety and profitability of mining operations. The following conclusions are drawn:

- A THMC backfill curing system has been developed for curing and monitoring CPB samples under controlled THMC conditions mimicking field conditions. This systems successfully reproduces loading conditions close to those in the field, demonstrating its suitability for subjecting laboratory CPB samples to realistic loading scenarios in the field.
- The THMC factors play a crucial role in both the generation and evolution of PWP within CPB. The findings underscore the substantial impact of both individual THMC factors and their interactions on the development of PWP within CPB. Results reveal that both individual THMC factors and their interactions significantly influences the onset and progression of PWP within CPB structures.
- The results highlight the importance of taking field drainage conditions (i.e. drained, undrained or partially drained) into account when assessing the PWP in the backfill structure and its overall geotechnical behavior and mechanical stability. The results obtained show that the PWP values in the drained CPB-PES materials are significantly lower than those in the partially drained and undrained CPB-PES samples. Moreover, drainage allows a much faster dissipation of the excess of PWP.
- It is found that non-isothermal curing temperatures in the field have a significant impact on

the magnitude of PWP generated in the backfill structure, as well as on the PWP dissipation rate. The results show a significant decrease in PWP values in CPB-PES exposed to higher field curing temperatures. In addition, higher curing temperatures accelerate the dissipation of excess PWP in the CPBs studied, which is beneficial for early barricade openings, i.e. for increasing mine productivity. The findings underscore the significance of taking into account elevated backfill field curing temperatures, when assessing the progression of PWP in backfill structure, which is essential for cost-effective design of the CPB and barricade structures.

- The results indicate that the vertical stresses to which CPB-PES structures are subjected during curing can significantly impact the PWP values inside the CPB and their evolution with time.
- The magnitude and evolution of PWP in CPB systems are intricately connected to the introduction of chemical additives, such as superplasticizers. The findings suggest that CPBs incorporating PES initially (at very early ages) demonstrate higher PWP levels than their counterparts without PES due to the retardation of cement hydration by PES. Nevertheless, with the passage of curing time, CPBs with PES exhibit higher rates of PWP dissipation or lower PWP levels, attributable to the enhanced cement hydration facilitated by PES. Considering these two contrasting effects of PES on the magnitude and evolution of water pressure within the CPB is vital for designing backfills that are both safe and cost-effective.

In summary, this research holds vital significance for the mining industry and backfill designers, offering essential technical insights into THMC factors affecting pore water pressure in CPB-PES. Understanding these interactions is crucial for optimizing CPB and barricade design, ensuring structural integrity, enhancing mine productivity, and informing future research on numerical models for predicting PWP in all CPB structures.

Funding National Natural Sciences and Engineering Research Council of Canada (NSERC).

Data Availability All data and materials or used during the study appear in the submitted article.

Code Availability Not applicable.

Declarations

Conflict of interest There are no known conflicts of interests or competing interests.

References

Alainachi I, Fall M, Majeed M (2022) Behaviour of backfill undergoing cementation under cyclic loading. Geotech Geol Eng 40:4735–4759. https://doi.org/10.1007/s10706-022-02181-y

Aldhafeeri Z, Fall M (2017) Sulphate induced changes in the reactivity of cemented tailings backfill. Int J Miner Process 166:13–23. https://doi.org/10.1016/j.minpro.2017.06.007

Al-Moselly Z, Fall M (2022) Effect of thermo-hydro-mechanical-chemical processes on the strength development of cemented paste backfill containing polycarboxylate ether-based superplasticizer. In: 75th Canadian geotechnical conference. Calgary, Canada

Al-Moselly Z, Fall M, Haruna S (2022) Further insight into the strength development of cemented paste backfill materials containing polycarboxylate ether-based superplasticizer. J Build Eng 47:103859. https://doi.org/10.1016/j.jobe.2021.103859

BASF (2015) MasterGlenium 7500 Full-range water-reducing admixture. https://www.master-builders-solutions.com/en-us/products/concrete-admixtures/water-reducers/water-reducers-high-range/masterglenium-7500

Belem T, Aatar OE, Bussière B et al (2006) Self-weight consolidation of column of cemented pastefill. In: 7th seminar on paste and thickened tailings. Irlande, p 13P

Bentz DP (2008) A review of early-age properties of cement-based materials. Cem Concr Res 38:196–204. https://doi.org/10.1016/j.cemconres.2007.09.005

Björnström J, Chandra S (2003) Effect of superplasticizers on the rheological properties of cements. Mater Struct Constr 36:685–692. https://doi.org/10.1617/13912

Cao S, Yilmaz E, Song W (2018) Evaluation of viscosity, strength and microstructural properties of cemented tailings backfill. Minerals 8:1–19. https://doi.org/10.3390/min8080352

Cavusoglu I, Fall M (2022) Engineering Properties of cemented paste backfill with full-range water-reducing admixture. SSRN Electron J. https://doi.org/10.2139/ssrn.4156513

Chai S, Zheng J, Li L (2023) Kink Effect on the stress distribution in 2D backfilled Stopes. Geotech Geol Eng 41:3225–3238. https://doi.org/10.1007/s10706-023-02434-4

Chen S, Wu A, Wang Y, Wang W (2021) Coupled effects of curing stress and curing temperature on mechanical and physical properties of cemented paste backfill. Constr Build Mater 273:121746. https://doi.org/10.1016/j.conbuildmat.2020.121746

Cui L, Fall M (2016) Multiphysics model for consolidation behaviour of cemented paste backfill. ACSE Int J Geomech 17(3):23

Cui L, Fall M (2017) Multiphysics modeling of arching effects in fill mass. Comput Geotech 83:114–131. https://doi.org/10.1016/j.compgeo.2016.10.021

Cui L, Fall M (2017) Multiphysics model for consolidation behavior of cemented paste backfill. Int J Geomech. https://doi.org/10.1061/(asce)gm.1943-5622.0000743

Cui L, Fall M (2017) Modeling of pressure on retaining structures for underground fill mass. Tunn Undergr Sp Technol 69:94–107. https://doi.org/10.1016/j.tust.2017.06.010

Cui L, Fall M (2018) Modeling of self-desiccation in a cemented backfill structure. Int J Numer Anal Methods Geomech 42:558–583. https://doi.org/10.1002/nag.2756

Cui L, Fall M (2018b) Multiphysics modeling and simulation of strength development and distribution in cemented tailings Backfill structures. Int J Concr Struct Mater. https://doi.org/10.1186/s40069-018-0250-y

Doherty JP, Hasan A, Suazo GH, Fourie A (2015) Investigation of some controllable factors that impact the stress state in cemented paste backfill. Can Geotech J 52:1901–1912. https://doi.org/10.1139/cgj-2014-0321

Ercikdi B, Cihangir F, Kesimal A et al (2010) Utilization of water-reducing admixtures in cemented paste backfill of sulphide-rich mill tailings. J Hazard Mater 179:940–946. https://doi.org/10.1016/j.jhazmat.2010.03.096

Fall M, Adrien D, Celestin JC, Pokharel M, Touré M (2009) Saturated hydraulic conductivity of cemented paste backfill. Miner Eng 22(15):1307–1317

Fall M, Célestin JC, Pokharel M, Touré M (2010) A contribution to understanding the effects of curing temperature on the mechanical properties of mine cemented tailings backfill. Eng Geol 114:397–413. https://doi.org/10.1016/j.enggeo.2010.05.016

Fall M, Célestin J, Sen HF (2010) Potential use of densified polymer-pastefill mixture as waste containment barrier materials. Waste Manag 30:2570–2578. https://doi.org/10.1016/j.wasman.2010.07.016

Fang K, Fall M (2019) Chemically induced changes in the shear behaviour of interface between rock and tailings backfill undergoing cementation. Rock Mech Rock Eng 52:3047–3062. https://doi.org/10.1007/s00603-019-01757-0

Fang K, Fall M (2020) Shear behavior of the interface between rock and cemented backfill: effect of curing stress, drainage condition and backfilling rate. Rock Mech Rock Eng 53:325–336. https://doi.org/10.1007/s00603-019-01909-2

Fang K, Fall M (2021) Shear behaviour of rock–tailings backfill interface: effect of cementation, rock type, and rock surface roughness. Geotech Geol Eng 39:1753–1770. https://doi.org/10.1007/s10706-020-01586-x

Ghirian A, Fall M (2013) Coupled thermo-hydro-mechanical-chemical behaviour of cemented paste backfill in column experiments. Part I: physical, hydraulic and thermal processes and characteristics. Eng Geol 164:195–207. https://doi.org/10.1016/j.enggeo.2013.01.015

Ghirian A, Fall M (2013) Experimental investigations of the thermo-hydro-mechanical-chemical behavior of cemented paste backfill. 23rd world mining congress and expo. Montreal, Canada, pp 11–15

Ghirian A, Fall M (2014) Coupled thermo-hydro-mechanical—chemical behaviour of cemented paste backfill in column experiments part II: mechanical, chemical and microstructural processes and characteristics. Eng Geol 170:11–23

Ghirian A, Fall M (2015) Coupled behavior of cemented paste backfill at early ages. Geotech Geol Eng 33:1141–1166. https://doi.org/10.1007/s10706-015-9892-6

Ghirian A, Fall M (2016) Strength evolution and deformation behaviour of cemented paste backfill at early ages: effect of curing stress, filling strategy and drainage. Int J Min Sci Technol 26:809–817. https://doi.org/10.1016/j.ijmst.2016.05.039

Haruna S, Fall M (2020) Strength Development of cemented tailings materials containing polycarboxylate ether-based Superplasticizer: experimental results on the Effect of Time and temperature. Can J Civ Eng. https://doi.org/10.1139/cjce-2019-0809

Haruna S, Fall M (2022) Reactivity of cemented paste backfill containing polycarboxylate-based superplasticizer. Min Eng 188:107856. https://doi.org/10.1016/j.mineng.2022.107856

Hasan A, Suazo G, Fourie AB (2013) Full scale experiments on the effectiveness of a drainage system for cemented paste backfill. In: Paste 2013. Jewell RJ, Fourie AB, Caldwell J, Pimenta J (eds), 2013 Australian centre for geomechanics, Perth, ISBN 978-0-9870937-6-9

Helinski M, Fourie A, Fahey M (2006) Mechanics of early age cemented Paste Backfill. In: Proceedings of ninth int semin paste thick tailings, pp 313–322. https://doi.org/10.36487/acg_repo/663_27

Helinski M, Fourie A, Fahey M, Ismail M (2007) Assessment of the self-desiccation process in cemented mine backfills. Can Geotech J 44:1148–1156. https://doi.org/10.1139/T07-051

Helinski M, Fahey M, Fourie A (2011) Behavior of cemented paste backfill in two mine stopes: measurements and modeling. J Geotech Geoenviron Eng 137:171–182. https://doi.org/10.1061/(asce)gt.1943-5606.0000418

Huang Z, Cao S, Qin S (2022) Research on the mechanical properties of 3D printing polymer reinforced cemented tailings Backfill under uniaxial compression. Geotech Geol Eng 40:3255–3266. https://doi.org/10.1007/s10706-022-02091-z

Hua C, Acker P, Ehrlacher A (1995) Analyses and models of the autogenous shrinkage of hardening cement paste. I. Modelling at macroscopic scale. Cem Concr Res 25:1457–1468. https://doi.org/10.1016/0008-8846(95)00140-8

Jiang H, Fall M, Li Y, Han J (2019) An experimental study on compressive behaviour of cemented rockfill. Constr Build Mater 213:10–19

Landriault D (2001) Backfill in underground mining. In: Hustrulid WA (ed) Underground mining methods engineering funda mentals and international case studies. SME, USA, pp 608–609

Lea F (1970) The chemistry of cement and concrete. Edward Arnold Ltd, London

Li W, Fall M (2016) Sulphate effect on the early age strength and self-desiccation of cemented paste backfill. Constr Build Mater 106:296–304. https://doi.org/10.1016/j.conbuildmat.2015.12.124

Li J, Yilmaz E, Cao S (2020) Influence of solid content, cement/tailings ratio, and curing time on rheology and strength of cemented tailings backfill. Minerals 10:1–14. https://doi.org/10.3390/min10100922

Lu G, Fall M (2018) Simulation of blast induced liquefaction susceptibility of subsurface fill mass. Geotech Geol Eng 36:1683–1706. https://doi.org/10.1007/s10706-017-0423-5

Mangane MBC, Argane R, Trauchessec R et al (2018) Influence of superplasticizers on mechanical properties and workability of cemented paste backfill. Min Eng 116:3–14. https://doi.org/10.1016/j.mineng.2017.11.006

McCarter WJ, Chrisp TM, Starrs G, Blewett J (2003) Characterization and monitoring of cement-based systems using intrinsic electrical property measurements. Cem Concr Res 33:197–206. https://doi.org/10.1016/S0008-8846(02)00824-4

Min C, Liu Z, Shi Y, Lu X (2023) Improving the strength performance of cemented phosphogypsum backfill with sulfate-resistant binders. Constr Build Mater 409:133974. https://doi.org/10.1016/j.conbuildmat.2023.133974

Morsy MS (1999) Effect of temperature on electrical conductivity of blended cement pastes. Cem Concr Res 29:603–606. https://doi.org/10.1016/S0008-8846(98)00198-7

Nasir O, Fall M (2009) Modeling the heat development in hydrating CPB structures. Comput Geotech 36:1207–1218. https://doi.org/10.1016/j.compgeo.2009.05.008

Orejarena L, Fall M (2008) Mechanical response of a mine composite material to extreme heat. Bull Eng Geol Environ 67:387–396. https://doi.org/10.1007/s10064-008-0148-z

Ouattara D, Yahia A, Mbonimpa M, Belem T (2017) Effects of superplasticizer on rheological properties of cemented paste backfills. Int J Miner Process 161:28–40. https://doi.org/10.1016/j.minpro.2017.02.003

Ouattara D, Mbonimpa M, Yahia A, Belem T (2018) Assessment of rheological parameters of high density cemented paste backfill mixtures incorporating superplasticizers. Constr Build Mater 190:294–307. https://doi.org/10.1016/j.conbuildmat.2018.09.066

Papayianni I, Tsohos G, Oikonomou N, Mavria P (2005) Influence of superplasticizer type and mix design parameters on the performance of them in concrete mixtures. Cem Concr Compos 27:217–222. https://doi.org/10.1016/j.cemconcomp.2004.02.010

Roshani A, Fall M (2020) Rheological properties of cemented paste backfill with nano-silica: link to curing temperature. Cem Concr Compos 114:103785. https://doi.org/10.1016/j.cemconcomp.2020.103785

Sakai E, Kasuga T, Sugiyama T et al (2006) Influence of superplasticizers on the hydration of cement and the pore structure of hardened cement. Cem Concr Res 36:2049–2053. https://doi.org/10.1016/j.cemconres.2006.08.003

Sari M, Yilmaz E, Kasap T, Guner NU (2022) Strength and microstructure evolution in cemented mine backfill with low and high pH pyritic tailings: Effect of mineral admixtures. Constr Build Mater 328:127109. https://doi.org/10.1016/j.conbuildmat.2022.127109

Sari M, Yilmaz E, Kasap T (2023) Long-term ageing characteristics of cemented paste backfill: usability of sand as a partial substitute of hazardous tailings. J Clean Prod 401:136723. https://doi.org/10.1016/j.jclepro.2023.136723

Shahsavari M, Grabinsky M (2015) Mine backfill porewater pressure dissipation: numerical predictions and field measurements. In: 68th proceedings Canadian geotechnical conference. Quebec City

Shahsavari M, Grabinsky M (2016) Pore Water pressure variations in cemented paste backfilled Stopes. Geo-Chicago. Chicago, Illinois, pp 331–342

Shahsavari M, Jafari M, Grabinsky M (2023) Simulation of cemented paste backfill (CPB) deposition through column experiments: comparisons of field measurements, laboratory measurements, and analytical solutions. Can Geotech J 60:1505–1514. https://doi.org/10.1139/cgj-2020-0597

Simms P, Grabinsky M (2009) Direct measurement of matric suction in triaxial tests on early-age cemented paste backfill. Can Geotech J 46:93–101. https://doi.org/10.1139/T08-098

Thompson BD, Grabinsky MW, Bawden WF, Counter DB (2009) In-situ measurements of cemented paste backfill in long-hole stopes. RockEng09 proc 3. CANUS Rock Mech Symp 2009:1–10

Thottarath S (2010) Electromagnetic characterization of cemented paste backfill in the field and laboratory. University of Toronto

Wang H, Qiao L (2019) Coupled effect of cement-to-Tailings ratio and solid content on the early age strength of cemented Coarse tailings Backfill. Geotech Geol Eng 37:2425–2435. https://doi.org/10.1007/s10706-018-00766-0

Wang Y, Fall M, Wu A (2016) Initial temperature-dependence of strength development and self-desiccation in cemented paste backfill that contains sodium silicate. Cem Concr Compos 67:101–110. https://doi.org/10.1016/j.cemconcomp.2016.01.005

Wang Y, Na Q, Yang J et al (2023) Monitoring of barricade pressure during the entire backfilling process for a high iron mine stope. Case Stud Constr Mater 19:e02456. https://doi.org/10.1016/j.cscm.2023.e02456

Wu D, Fall M, Cai S (2012) Coupled modeling of temperature distribution and evolution in cemented tailings Backfill structures that contain mineral admixtures. Geotech Geol Eng 30:935–961. https://doi.org/10.1007/s10706-012-9518-1

Wu D, Fall M, Cai SJ (2013) Coupling temperature, cement hydration and rheological behaviour of fresh cemented paste backfill. Min Eng 42:76–87. https://doi.org/10.1016/j.mineng.2012.11.011

Wu D, Fall M, Cai S (2014) Numerical modelling of thermally and hydraulically coupled processes in hydrating cemented tailings backfill columns. Int J Min Reclam Environ 28:173–199. https://doi.org/10.1080/17480930.2013.809194

Wu D, Zhao R, Qu C (2019) Effect of curing temperature on mechanical performance and acoustic emission properties of cemented coal gangue-fly Ash Backfill. Geotech Geol Eng 37:3241–3253. https://doi.org/10.1007/s10706-019-00839-8

Yan R, Yin S, Zhang H et al (2023) Effect of superplasticizer on the setting behaviors and mechanical properties of tailings-waste rock cemented paste backfills. Case Stud Constr Mater 18:e01714. https://doi.org/10.1016/j.cscm.2022.e01714

Yilmaz E, Kesimal A, Ercikdi B, Alp I (2003) Determination of the optimum cement content for paste backfill samples.

In: 8th international mining congress and exhibition of Turkey IMCET. Antalya, Turkey, pp 119–126
Yilmaz E, Benzaazoua M, Belem T, Bussière B (2009) Effect of curing under pressure on compressive strength development of cemented paste backfill. Min Eng 22:772–785. https://doi.org/10.1016/j.mineng.2009.02.002
Yilmaz E, Belem T, Benzaazoua M (2012) One-dimensional consolidation parameters of cemented paste backfills. Min Resour Manag 28:29–45. https://doi.org/10.2478/v10269-012-0030-2
Yilmaz E, Cao S (2022) Wu D (2022) Advances in the design and implementation of cementitious backfills. Frontiers in Materials 9:964111
Yoshioka K, Sakai E, Daimon M, Kitahara A (1997) Role of steric hindrance in the performance of superplasticizers for concrete. J Am Ceram Soc 80:2667–2671. https://doi.org/10.1111/j.1151-2916.1997.tb03169.x
Zhang Z, Su H, Guan W (2022) Study on the geological environmental disturbance and reclamation technology of underground coal mines: a case study, Xinjiang, China. Geotech Geol Eng 41:1725–1739
Zhang D, Wang J, Guo S, Cao J (2022) Numerical simulation of crack evolution mechanism and subsidence characteristics effected by rock mass structure in block caving mining. Geotech Geol Eng 40:5377–5395. https://doi.org/10.1007/s10706-022-02220-8
Zhao X, Fourie A, Veenstra R, Qi C (2020) Safety of barricades in cemented paste-backfilled stopes. Int J Miner Metall Mater 27:1054–1064. https://doi.org/10.1007/s12613-020-2006-3
Zhou Q, Beaudoin JJ (2003) Effect of applied hydrostatic stress on the hydration of Portland cement and C3S. Adv Cem Res 15:9–16. https://doi.org/10.1680/adcr.2003.15.1.9